Immunity, Vol. 9, 199–208, August, 1998, Copyright ©1998 by Cell Press

The Crystal Structure of H-2D^d MHC Class I Complexed with the HIV-1-Derived Peptide P18-I10 at 2.4 Å Resolution: Implications for T Cell and NK Cell Recognition

Adnane Achour,*# Karina Persson,†# Robert A. Harris,*‡ Jonas Sundbäck,* Charles L. Sentman,§ Ylva Lindqvist,† Gunter Schneider,† and Klas Kärre*‖
*Microbiology and Tumor Biology Center
†Department of Medical Biochemistry and Biophysics
‡Center for Molecular Medicine
Karolinska Hospital
Stockholm
Sweden
§Umeå Center for Molecular Pathogenesis
Umeå University
Umeå
Sweden

Summary

The structure of H-2D^d complexed with the HIV-derived peptide P18-I10 (RGPGRAFVTI) has been determined by X-ray crystallography at 2.4 Å resolution. This MHC class I molecule has an unusual binding motif with four anchor residues in the peptide (G2, P3, R/K/H5, and I/L/F9 or 10). The cleft architecture of H-2D^d includes a deep narrow passage accomodating the N-terminal part of the peptide, explaining the obligatory G2P3 anchor motif. Toward the C-terminal half of the peptide, p5R to p8V form a type I′ reverse turn; residues p6A to p9T, and in particular p7F, are readily exposed. The structure is discussed in relation to functional data available for T cell and natural killer cell recognition of the H-2D^d molecule.

Introduction

Class I major histocompatibility complex (MHC) molecules are plasma membrane proteins expressed by virtually all mammalian cells. They transport peptides to the cell surface for presentation to T cells of the immune system. MHC class I molecules are composed of two subunits: the polymorphic membrane-anchored heavy chain (with extracellular domains α_1, α_2, and α_3) and a lighter invariant soluble noncovalently attached β_2-microglobulin (β_2m) unit. The third component of the MHC complex is an 8- to 11-amino acid–long peptide positioned in a cleft formed by the α_1 and β2 domains of the heavy chain.

Recognition of peptides complexed to MHC molecules by T cell receptors is a critical event in initiation of an immune response (Zinkernagel and Doherty, 1974; Haskins et al., 1984; Townsend et al., 1986; Bjorkman and Parham, 1990). Invasion of a cell by a pathogen results, in most cases, in presentation of non-self-antigens on the cell surface by MHC class I molecules, which can activate T lymphocytes. Each allelic form of an MHC class I molecule is capable of binding a diverse series of peptides, and this capacity, coupled with variations in the peptide binding specificities of the different alleles, generates the broad sampling of peptide epitopes necessary for a cellular immune function.

HLA-A2 was the first crystal structure of an MHC complex to be determined (Bjorkman et al., 1987a, 1997b), soon followed by the structures of murine and human MHC molecules complexed with single peptides (reviewed in Jones, 1997). However, the structure of H-2D^d is unknown. A structural analysis of this particular MHC class I molecule is important for several reasons. First, sequencing of peptide pools eluted from H-2D^d (Corr et al., 1993; Rammensee et al., 1995) has revealed an unusual type of peptide binding motif, requiring three principal anchor residues (p2G, p3P, and p10I/L/F) and a very strong secondary anchor position in the middle of the peptide (p5R/K/H). Second, the H-2D^d molecule has been extensively used in functional analysis of T cell recognition, particularly in presentation of the P18-I10 peptide RGPGRAFVTI from the V3-loop of the gp160 HIV-1 protein. This peptide sequence may be of particular interest in comparative structural studies since it displays "promiscuous" binding to four different murine (H-2D^d, H-2D^p, H-2^u, and H-2^q; Shirai et al., 1992) and at least one human (HLA-A2; Alexander-Miller et al., 1996) MHC class I molecules. Furthermore, there are CTL (cytotoxic T lymphocyte) clones that can respond to the peptide whether it is presented by H-2D^d, H-2D^p, or H-2^u class I molecules (Shirai et al., 1993, 1996, 1997). The structure of H-2D^d complexed with P18-I10 may help to define the structural basis for this "degeneracy" of the MHC specificity and cross-reactivity of T cell responses.

Finally and most importantly, the H-2D^d molecule represents the prototype ligand for the best characterized natural killer (NK) cell receptor, Ly-49A. It is now clear that MHC class I molecules play an important role in the regulation of NK cell activity (Kärre, 1985; Kärre et al., 1986; Ljunggren and Kärre, 1990; Gumperz and Parham, 1995). Novel types of inhibitory receptors on NK cells can recognize MHC class I complexes (Karlhofer et al., 1992; Moretta et al., 1993; Litwin et al., 1994; Long et al., 1997; Ryan and Seaman, 1997). Expression of an appropriate MHC class I molecule on the surface of a cell will prevent its destruction by NK cells through an inhibitory effect following the engagement of the target cell MHC molecule by the NK cell receptor. In the mouse, this is mediated by receptors of the Ly-49 family within the superfamily of C-type lectins. Ly-49A can recognize H-2D^d, H-2D^k, and H-2D^p molecules but not any of the allelic MHC class I products that have been crystallized to date (Karlhofer et al., 1992; Brennan et al., 1994; Daniels et al., 1994a; Kane, 1994; Sentman et al., 1994; Alheim-Olsson and Kärre, unpublished data). Inhibitory recognition by Ly-49A maps to the $\alpha_1\alpha_2$ domains of the MHC class I ligand (Karlhofer et al., 1992; Sundbäck et al., 1998); it requires that the H-2D^d molecule has bound a peptide, but there is no specificity since any peptide bound to H-2D^d will permit recognition (Correa and

‖ To whom correspondence should be addressed (e-mail: klas.karre@mtc.ki.se).
# These authors contributed equally to this work.

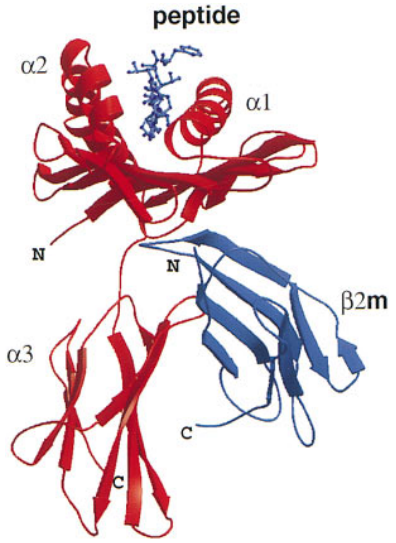

Figure 1. Schematic View of the H-2D^d Complex

The α and β chains are depicted in red and blue, respectively. The bound P18-I10 decapeptide is shown in a ball and stick representation. The figure was created using the Molscript program (Kraulis, 1991).

Raulet, 1995; Orihuela et al., 1996). Ly-49A can bind to different sugars (Daniels et al., 1994b), but the carbohydrates of the MHC class I molecule are not necessary for the recognition of H-2D^d by Ly-49A (Matsumoto et al., 1998).

The purpose of this study was to establish a structural basis for understanding the various interesting functional features of the H-2D^d molecule. We have employed a bacterial expression system and in vitro complex formation for crystallization of H-2D^d with the HIV-1 peptide RGPGRAFVTI (Achour et al., 1998). We now report the crystal structure at 2.4 Å resolution, and the refined model is analyzed with respect to peptide binding and T cell and NK cell recognition.

Results and Discussion

Overall Structure of the H-2D^d Complex

The overall backbone structure of the recombinant H-2D^d is presented in Figure 1. As expected from the high degree of sequence identity, it is very similar to the previously reported mouse and human MHC crystal structures, e.g., the r.m.s. deviation between H-2D^d and the crystal structure of H-2D^b (Young et al., 1994) for all Cα atoms in the heavy chain and the β_2m subunit is 1.23 Å as calculated with the O program (Jones et al., 1991). The structure was determined by molecular replacement using X-ray diffraction data to 2.4 Å resolution. The R value for the refined model with good stereochemistry is 27.8%, and R_{free} is 32.3%. The final electron density map is of excellent quality (Figure 2) despite a high average B factor in the crystals. There are no ambiguities in the structure, except for a few surface side chains. The residues that constitute the CD8 binding part of the α_3 domain (amino acids 220–229) (Gao et al., 1997), residues 105–107, and parts of the region comprising residues 132–152 in the α_2 domain, have weak electron density, reflecting higher than average flexibility for this part of the molecule. However, the electron density for all residues in contact with the peptide is clearly defined.

The orientation of the β_2m subunit with respect to the heavy chain was analyzed with the TOP program (Lu, 1996) and compared to other MHC class I complexes. The orientation of the β_2m chain in the H-2D^d structure is very similar, within 2 to 4°, to that of H-2D^b and the human MHC class I molecules. A significantly larger difference in this respect was apparent between H-2D^d and H-2K^b; the orientation of the β_2m subunits deviates by approximately 10° in these two MHC class I molecules. The hydrogen bonding pattern and van der Waals contacts between β_2m and the H-2D^d heavy chain were compared with the corresponding interactions in H-2D^b, H-2K^b, and H-2L^d (Young et al., 1994; Balendiran et al., 1997). The number of intersubunit contacts in H-2D^d is comparable to that found in H-2D^b (data not shown). This correlates with the higher stability of these class I molecules as compared to H-2L^d, which exhibits much fewer contacts (Balendiran et al., 1997).

Conformation and Length of the Bound Peptide—Influence of Unusual Features of the H-2D^d Binding Cleft

While peptides binding to H-2K^b and H-2D^b are 8–9 amino acids long, those that bind to H-2D^d (with a few exceptions) are at least nine amino acids long, and many of them are decamers (Corr et al., 1993). The conformation and minimal length of peptides bound by an MHC class I molecule is determined by the distance between the two hydrogen bonding networks used for anchoring of the peptide N and C termini and by the mid-cleft architecture (Bouvier and Wiley, 1994; Young et al., 1995). The H-2D^d peptide binding cleft can be divided into three regions (Figure 3): a narrow deep cleft binding the N-terminal part of the peptide, a more shallow broad mid-cleft depression over which amino acids 5–9 of the peptide are positioned, and the characteristic deep hydrophobic F pocket. The first two regions of the cleft are separated by the simultaneous presence, unique for H-2D^d (Watts et al., 1989), of two tryptophans at positions W97 and W114. The tryptophan residues create a wall that the peptide has to climb from the deep cleft to the shallow part of the binding cleft (Figure 3). This plateau harbors an auxiliary anchor position at p5, forcing the remainder of the peptide to arch out of the cleft before anchoring at the C terminus. This architecture requires a minimum of a nonamer for binding; five residues are needed to reach from the N terminus over the wall to the p5 anchor position and then four amino acids to reach the F pocket.

Figures 2A and 3 depict the conformation of the peptide (RGPGRAFVTI) when bound to H-2D^d. It binds in the cleft along the α_1-helix in a hitherto unobserved conformation. The N terminus binds strongly through hydrogen bonds to the side chains of Y171 and Y7 in the A pocket, and the C-terminal is anchored by a network of hydrogen bonds formed by Y84, T143, and K146 in the F pocket (Table 1), similarly to other peptides in MHC class I complexes (Madden, 1995; Young et al., 1995). However, the peptide residues p5R to p8V form a reverse

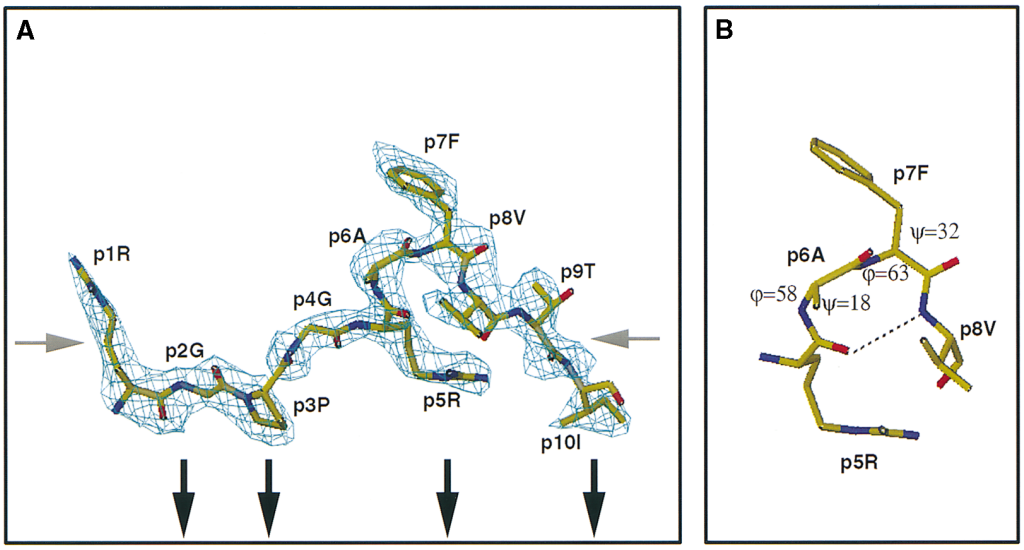

Figure 2. Conformation of the Bound Peptide

(A) Side view of the peptide RGPGRAFVTI colored according to atom type in a σ_A-weighted |Fo-Fc| annealed omit map at 2σ contour level. The peptide N terminus to C terminus main chain direction runs left to right, illustrating the anchor positions (perpendicular arrows) and the emerging side chains that can interact with, e.g., T cell receptors. The part of the peptide that protrudes above the surface of the protein is indicated by the horizontal arrows on each side of the peptide. The figure was created using the O program (Jones et al., 1991).

(B) Residues P5R to P8V of the bound peptide, illustrating the reverse type I′ turn in the peptide. The phi, psi angles and the hydrogen bond characteristic for this type of turn are indicated.

turn of type I′ over the mid-cleft depression (Figure 2B). In general, such turns are characterized by four consecutive residues, often with a hydrogen bond between the main chain atoms of residue i and i + 3. The type of turn is defined by the pair of phi/psi angles of residues i + 1 and i + 2 (Wilmot et al., 1990). The turn of the bound peptide is stabilized by a hydrogen bond between the carboxyl group of p5R and the amino group of p8V. The phi and psi values of the residues located in between p6A and p7F are 58°/18° and 63°/32°, respectively, corresponding to a β-turn of type I′ (γ γ). As a consequence of this structural feature, residues p6A to p9T and in particular p7F are exposed to solvent (Figures 2 and 3).

The presence of this β-turn probably confers additional stability to bound decamer peptides that have to bulge between p5R and p10I anchor binding locations. It is probably not required for the binding of nonamers and thus probably not a general feature of peptides bound to H-2D^d.

Structural Features Explaining the Shared Motif of H-2D^d Binding Peptides

The architecture of the H-2D^d binding cleft explains the unusual motif with four anchor positions used by peptides for binding (Corr et al., 1993). The peptide binds to the cleft through two anchor positions on each side

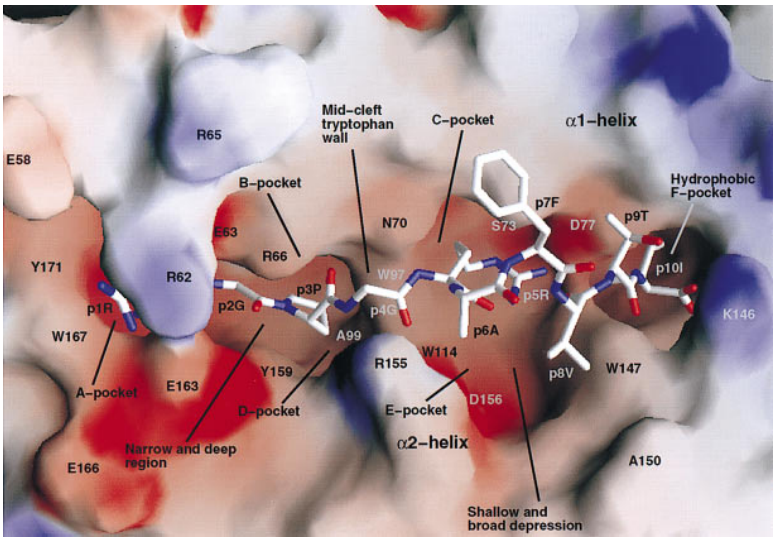

Figure 3. The Peptide P18-I10 (RGPGRAF VTI) Bound to the Cleft of the MHC Class I H-2D^d Molecule

The peptide is represented as a stick model, while the MHC class I molecule is represented by its surface (viewed from above). The regions specific for the binding of different sections of the peptide are displayed. The position of H-2D^d residues important for the binding of P18-I10 and a few other residues are indicated. Negatively charged regions of the surface are given in red and positively charged regions in blue, with a scale from −15 kT to +15 kT. Peptide residue labels begin with p. It should be noted that R62 and E163 do not form significant electrostatic interactions; the closest distance between their side chains is 4.9 Å. This figure was created using the Grasp program (Nicholls et al., 1991).

Table 1. Hydrogen Bond (<3.2 Å) and van der Waals (<3.6 Å) Interactions of the Decapeptide P18–I10 with Residues of the Cleft in the H-2D^d Complex[a]

	Hydrogen Bonding			
Peptide Residue	Atom	Atom	H-2D^d-residue	Van der Waals Contacts[b]
p1R	N	OH	Y171	W167 (5), R62 (11),
	N	OH	Y7	E63 (1), E163 (2), Y7 (6),
	O	OH	Y159	Y159 (3), Y171 (4)
	NH1	OE1	E163	
p2G	N	OE1	E63	Y7 (4), E63 (1), R66 (7), Y159 (2)
p3P	O	NH1	R66	R66 (3), Y159 (1), W97 (1), N70 (1)
	O	ND2	N70	
p4G	O	NH2	R155	R155 (4)
p5R	N	OD1	N70	N70 (2), D77 (2)
	NH1		Wat32	Wat32 (2)
	NH2	OD2	D77	
p6A	None			None
p7F	None			None
p8V	None			W147(2)
p9T	O	NE1	W147	V76 (1), D77 (4), W147 (4)
p10I	N	OD1	D77	D77 (8), Y84 (4),
	O	OG1	T143	T143 (4), K146 (2)
	O	OH	Y84	
	OXT	NZ	K146	

[a] The analysis was performed with the Contacts program contained in the CCP4 suite (CCP4, 1994).
[b] Contacts of <3.6 Å between peptide and H-2D^d are listed with their numbers in parentheses.

of the tryptophan wall. Anchor positions p2G and p3P of the peptide bind in the deep N-terminal cleft, the basic residue p5R binds to the shallow, predominantly negatively charged depression, and the hydrophobic amino acid p10I at the C-terminal end of the peptide binds in the F pocket, similarly to pC-terminal binding in several other MHC class I molecules (Madden, 1995).

Of the 182 residues in the α_1/α_2 domain of the H-2D^d molecule, 15 interact through a hydrogen bond with the peptide. In addition, the peptide forms a large number of van der Waals interactions to protein atoms (Table 1). The reverse turn conformation of the P18-I10 peptide also gives rise to internal interactions between residues within the peptide (data not shown).

The Structure of the Deep, Narrow pN-Terminal Part of the Cleft Explains the Requirement for p2Gp3P in the Peptide

Both p2G and p3P are required for the peptide to bind; a mutation of either one of these amino acids impairs binding to the H-2D^d molecule (Takeshita et al., 1995). The H-2D^d crystal structure explains this obligatory motif; the GP combination at positions 2 and 3 is necessary for the peptide to meet the steric constraints in the cleft (Figures 3 and 4). The passage between R66 and E63 on the α_1-helix and Y159 on the α_2-helix is very narrow due to the side chain of R66 in the α_1 helix that projects down into the cleft. It interacts with the side chains of E24, Y45, and E63 and fills the B pocket normally present in other MHC class I molecules (Madden, 1995; Young et al., 1995). As a direct consequence of this narrow passage, no amino acid other than glycine can be allowed at this position of the peptide (Figure 4A). The glycine perfectly fills the cleft, leaving only 5% of its surface available to the solvent (4 Å^2). A mutation, e.g., to alanine, would result in a steric clash with the side chain of R66.

Proline, the second essential amino acid for binding of the peptide (Corr et al., 1993; Takeshita et al., 1995), is buried in the hydrophobic pocket formed by Y7, V9, W97, A99, W114, and Y159 (Figure 4B). No part of its side chain is accessible to the solvent. The proline ring stacks to the ring of Y159, the conformation of the tyrosine being stabilized through a hydrogen bond from its hydroxyl to the carbonyl oxygen of p1R. The backbone carbonyl of p3P binds strongly through two hydrogen bonds to R66 and N70.

The ψ value of the GP peptide bond lies in the β-region at around 180° in the Ramachandran plot. Any other ψ value would result in a steric clash against either R66 and E63 or Y159. The GP motif is thus necessary to provide a perfect fit for the peptide to the deep and narrow N-terminal cleft. Besides providing specific binding interactions as described above, p3P restrains the conformational freedom of the glycine anchor position (p2G) that precedes it. At the same time, this part of the peptide has a conformation, often adopted by GP units (MacArthur and Thornton, 1991), that allows the remaining part of the peptide to ascend the wall created by W97 and W114 to the shallow part of the cleft.

p5R Binds in the Shallow and Broad Depression

The cleft broadens in the shallow part of the binding groove between S73, D77, and D156. By contrast to MHC class I molecules H-2D^b (Young et al., 1994) and H-2L^d (Balendiran et al., 1997), there is no hydrophobic ridge crossing the cleft (Figure 5). The side chain of anchor position 5 rests on the shallow depression, a flat plateau formed by W114, W97, F116, and F74 from the α_1-helix and W147 from the α_2-helix (Figure 3). The positively charged guanidinium group of p5R interacts with the side chain of D77 (Table 1) and possibly through a net of hydrogen-bonded water molecules with D156. p5R also forms a hydrogen bond from its main chain

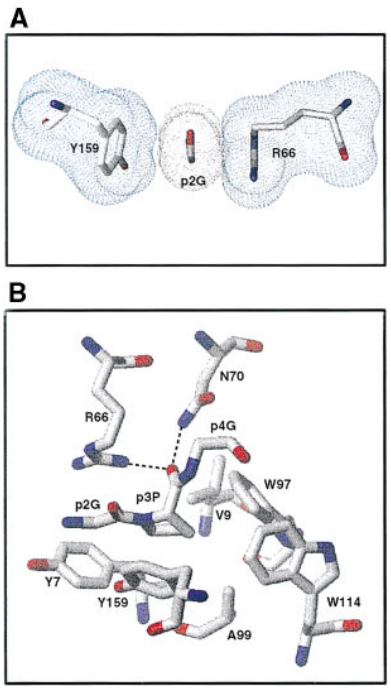

Figure 4. Interaction of the GP Anchor Motif in the Binding Cleft

(A) p2G is the only amino acid that fits in the narrow passage between R66 and Y159. The van der Waals surfaces of R66 and Y159 are colored in blue, while the van der Waals surface of p2G is colored in gray (section across the cleft, viewed from the C terminus of the peptide).

(B) The side chain of p3P is situated in a hydrophobic pocket formed by the side chains of V9, W97, A99, W114, and Y159 that stacks with its aromatic ring to p3P. The carbonyl of p3P binds through hydrogen bonds (depicted as broken lines) to the side chains of R66 and N70. The figure was created using the Grasp program (Nicholls et al., 1991). The color of the atoms is red for oxygen, blue for nitrogen, and white for carbon.

amino group to the side chain oxygen of N70. The side chain of this auxiliary anchor position is entirely covered by the remaining part of the peptide that bulges out over it, with the four following residues more or less exposed to the solvent. Only 3% of p5R is accessible to the solvent (5 Å^2). p5R also forms internal hydrogen bonds to side and main chain atoms of the peptide (Figure 2B; data not shown). This anchor position does not bind in a deep pocket, which may explain why the peptide is still able to bind when p5R is mutated to an alanine (Takeshita et al., 1995). p5R, H or K as in some other H-2D^d binding peptides, can thus be classified as a secondary anchor position (Corr et al., 1993) that helps to stabilize the nonameric and decameric peptides in their binding to H-2D^d, particularly through their interaction with the side chain of D77.

P10I Binds in the Hydrophobic F Pocket

The last anchor residue is a hydrophobic residue in accordance with the usual motif described in murine MHC class I molecules (Falk et al., 1991; Rammensee et al., 1995). In this case, it is an isoleucine that binds deeply (0% solvent accessibility) into the hydrophobic F pocket formed by residues Y123, F116, I124, W147, L95, and Y84, but the peptide can also have a leucine or a phenylalanine (Corr et al., 1993) at this position. In H-2D^d, the F pocket is wider than usual due to the presence of an alanine at position 81, in contrast to a leucine in most of the H-2 molecules (Watts et al., 1989).

Peptide Side Chains Protrude Toward the Solvent in Two Regions

Two parts of the peptide are exposed to solvent, the side chain of p1R and, more prominently, residues p6A, p7F, p8V, and p9T over the shallow and broad part of the binding groove (Figures 2 and 3). A study of the peptides eluted from H-2D^d complexes reveals a great diversity of amino acids in both regions (Corr et al., 1993).

The side chain of p1R projects out into the solvent (11% accessible to the solvent, 34 Å^2) and is held through planar stacking interactions with R62 and the aromatic side chain of W167 and through a hydrogen bond with E163. This part of the binding cleft is wide enough to accomodate other side chains.

The second part of the peptide that protrudes out of the cleft comprises positions p4G (21% solvent accessibility, 15 Å^2), p6A (68%, 54 Å^2), p7F (75%, 151 Å^2), p8V (42%, 39 Å^2), and p9T (26%, 30 Å^2). The side chains of the phenylalanine at position 7 and the threonine at position 9 are directed toward the α_1 part of the binding cleft, while the alanine at position 6 and the valine at position 8 are directed towards the α_2-helix (Figure 3).

On the α_2 part of the binding cleft, p6A is exposed to the solvent but makes hydrophobic interactions with the side chains of R155 and the side chain of p8V. The side chain of p8V forms hydrophobic interactions to a cluster composed by the side chains of W147, A150, and A152. p8V also forms internal main chain/main chain and main chain/side chain hydrogen bonds to p5R. On the α_1 side of the binding cleft, p7F covers all or parts of the side chains of G69, N70, and S73. The exposed side chain of p9T forms a hydrophobic interaction with the side chain of V76, while its main chain carbonyl interacts through a hydrogen bond to the side chain of W147.

The crystal structure is not consistent with the model of the MHC class I H-2D^d/P18-I10 complex that has been suggested previously (Corr et al., 1993) and that has been used for interpretation of functional data (Takeshita et al., 1995; Shirai et al., 1997; Matsumoto et al., 1998). These differences include (1) the way in which the peptide binds, e.g., p5R binds to D77 on the α_1 domain and not, as proposed in the model, to D156 on the α_2 domain; (2) spatial position of side chains, e.g., R66, a central amino acid in the binding of p2G, projects down in the crystal structure while it has been proposed to build a bridge over the P18-I10 peptide in the model; and (3) the way by which different potential epitopic side chains of the peptide are presented, e.g., p7F is exposed to the solvent and does not participate in binding of the peptide to the groove.

Implications of the Structure for Interpretation of Studies of Peptide Binding and T Cell Recognition

Functional studies (Takeshita et al., 1995), using alanine-substituted P18-I10 peptide variants, revealed that position p10I seemed to be the most critical for binding to H-2D^d, followed by p2G, p3P, and p5R. This sequence of

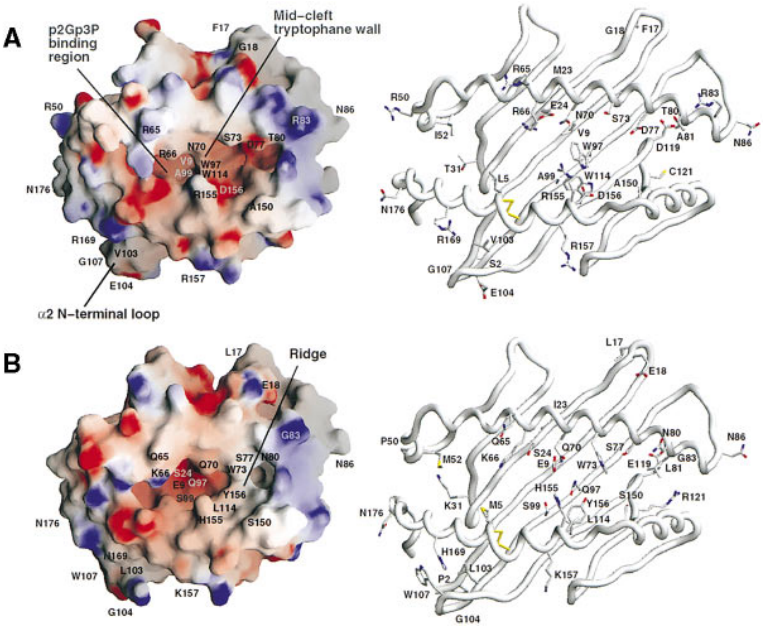

Figure 5. Differences in Side Chain Compositions of the H-2D^d and H-2D^b $\alpha_1\alpha_2$ Regions

(A) and (B) depict H-2D^d and H-2D^b, respectively. On the right part of the figure, the backbone of both MHC class I molecules is represented as a rod with only differences in side chains depicted. The latter are colored as follows: red for oxygen, blue for nitrogen, white for carbon, and yellow for sulfur. This part of the figure was created using the Setor program (Evans, 1993). On the left side, using the Grasp program (Nicholls et al., 1991), the differences between H-2D^d and H-2D^b in the resulting architecture in the $\alpha_1\alpha_2$ region are illustrated. Color and scale as in Figure 3. Interesting regions in both MHC class I molecules are depicted by arrows. The figures of H-2D^b were based on the crystal structure resolved by Young et al. (1994).

critical residues agrees with the motif already described (Corr et al., 1993) and with the crystal structure of the complex presented here; all four anchor residues become buried upon binding to H-2D^d providing large and specific binding energy. Positions 1, 4, 6, 7, 8, and 9 are exposed to the solvent. The most prominent of these residues, at positions 6, 7, and 8 of the peptide, have all been demonstrated to be T cell epitopic positions in the context of H-2D^d (Takahashi et al., 1989a, 1989b, 1992; Shirai et al., 1992, 1997; Takeshita et al., 1995). The substitution of p7F to an alanine did not impair binding or recognition by specific T cells, while substitution of the same position to an isoleucine prevented recognition (Takeshita et al., 1995). From the structure, we can conclude that this is not due to loss of binding of the peptide to H-2D^d but must be due to impaired interactions with the TCR.

The promiscuous MHC binding observed with the decamer P18-I10 (Shirai et al., 1992) implies that this peptide may possess structural features that confer broad binding specificity. No consensus peptide motif is known for H-2D^p, H-2^u, and H-2^q class I molecules. It is highly probable, however, that P18-I10 binds to these MHC molecules in a different manner than to H-2D^d, since many of the residues responsible for the binding of the anchor positions of P18-I10 differ between H-2D^d and the cross-binding MHC class I molecules. For example, position R66, important in forming the binding pocket for p2G and p3P in the case of H-2D^d, is occupied by asparagine and isoleucine, respectively, in the case of H-2D^p and H-2D/L^q. Furthermore, residue A99, unique for H-2D^d and important for the binding of p3P, is replaced by an arginine in the case of H-2D^p and a tyrosine in the case of H-2D^q and H-2L^q. The important middle wall composed by W97 and W114 in H-2D^d is replaced by G97 and E114 in H-2D^p and by R97 and E114 in H-2D^q and H-2L^q. D156 is substituted for L156 in H-2D^p and Y156 in H-2D^q and H-2L^q, rendering the equivalent binding of a large positively charged amino acid such as p5R difficult. In conclusion, analysis of the H-2D^d crystal structure combined with sequence comparisons indicates that the peptide has to bind in a different manner in the three other MHC class I molecules.

In spite of this, there are examples of CTL clones that cross-react with respect to the restriction element, i.e., they can recognize the peptide presented by different class I molecules (Shirai et al., 1992, 1997). Crystal structures of TCR complexed with MHC class I molecules (Garboczi et al., 1996; Garcia et al., 1996) reveal that the TCR simultaneously contacts residues on both the peptide and the MHC molecule. In the case of P18-I10 recognition, this could mean that the cross-recognizing TCR binds a part of the MHC class I molecule that is highly conserved between all of the cross-reacting alleles (H-2D^d, H-2D^p, and at least one of the class I locus products of the H-2^u haplotype) or that it is extremely sensitive to some side chains from the peptide such as p7F. These two possibilities are not mutually exclusive, and there is support for both of them. First, a study based on single amino acid substitutions of P18-I10 identified P7F, followed by p8V and p9T, as key residues in the recognition of P18-I10 presented by H-2D^d, H-2D^p, and by H-2^u class I molecules (Shirai et al., 1997). Second, a comparison of the amino acid sequences for H-2D^d and H-2D^p reveals interesting conserved regions, and the crystal structure indicates that they are all close to p7F. For example, E71, Q72, R75, and R79 are common to the two class I molecules and could thus be involved in the cross-recognition. There may be corresponding regions on the TCR side, since there is a preferential usage of Vβ8 in T cell clones recognizing P18-I10 in H-2D^d, H-2D^p, and H-2^u (Shirai et al., 1993). In conclusion, residues of the class I molecule and the p7F may form a "supermotif," preferentially recognized by TCR-Vβ8. Whether or not the reverse type I′ β-turn is present when the peptide is bound to H-2D^p and the relevant class I product of H-2^u, p7F might still be presented to the T cell receptor in a similar way as in H-2D^d.

Bidirectional cross-reactivity between the 15-mer peptide P18 and a nonhomologous gp160 15-mer peptide, HP53, has also been observed for CD8$^+$ CTL in strains expressing H-2D^d. This phenomenon was mapped to P18-I10 of P18 and to an eight-residue core of HP53, HP53-I8, VQGAYRAI (Shirai et al., 1996). In our analysis of the structure above, we have concluded that the cleft architecture of H-2D^d requires at least nonameric peptides, containing p2Gp3P as an obligatory motif, for binding from the A to the F pocket. HP53-I8 is an octamer and lacks p2Gp3P. We therefore propose that this peptide binds with one sole anchor position p8I in the deep F pocket. P5Y would then be in an equivalent position to p7F in P18-I10, known to be involved in TCR recognition, and the structural similarity in these side chains could then explain the cross-reactivity. This would not require the presence of a type I′ β-turn. Ongoing structural studies of other MHC class I molecules binding P18-I10 and HP53-I8 should help to better define the causes for this broad cross-recognition. It should be noted that among peptides eluted from H-2D^d, selected for strong binding in vivo, 20 out of 22 contained the p2Gp3P motif (Corr et al., 1993). Such peptides therefore appear superior in competing for loading into H-2D^d molecules in vivo.

H-2D^d As a Ligand for the NK Cell Receptor Ly-49A—Comparison with Other MHC Class I Molecules

H-2D^d, H-2D^k, and H-2D^p act as ligands for inhibitory recognition by the NK cell receptor Ly-49A, while H-2K^b, H-2L^d, H-2K^d, and H-2D^b fail to do so or at best represent weak ligands (Karlhofer et al., 1992; Kane, 1994; Ryan and Seaman, 1997; Takei et al., 1997; Kärre, unpublished data). Loading of H-2D^d molecules with the HIV-derived peptide RGPGRAFVTI, used by us for crystallization, or any of eight other H-2D^d binding peptides enabled recognition and inhibition through Ly-49A (Correa and Raulet, 1995; Orihuela et al., 1996). Loading of H-2D^b molecules with the influenza-derived peptide ASNEN METM did not result in inhibitory recognition by Ly-49A$^+$ NK cells.

To investigate structural features important for MHC class I recognition by the NK cell receptor Ly-49A, we thus compared the H-2D^d/RGPGRAFVTI structure with the published structure of H-2D^b complexed to the peptide ASNENMETM (Young et al., 1994) (Figure 5). We will focus our discussion of this comparison on differences in the α_2 domain (amino acids 90–182) of the molecule and particularly of its N-terminal part, for the following reasons. A recent study based on H-2D^d/D^b chimeric molecules has mapped allelic specificity of the Ly-49A receptor to the α_2 domain of the H-2D^d molecule (Sundbäck et al., 1998). Furthermore, 34-5-8S, the only anti-H-2D^d antibody that is capable of blocking the interaction between this MHC class I molecule and the Ly-49A receptor, binds to residues 92 to 116 in the N-terminal part of the α_2 domain (Abastado et al., 1987; Karlhofer et al., 1992; Orihuela et al., 1996).

There are 31 differences altogether in the amino acid sequences between the $\alpha_1\alpha_2$ domains of H-2D^d and H-2D^b (Watts et al., 1989); 13 of these are in the α_2 domain. In our analysis of these in relation to the structure, as well as sequences and models of other MHC class I molecules, two potential regions for Ly-49A recognition have emerged: the N-terminal-central part of the peptide binding groove with adjacent areas and an area around one of the N-specific glycosylation sites N176, including an external loop of the α_2 domain.

Central α_2 domain residues in the first region are A99, W97, and W114, all involved in the binding of the double p2Gp3P anchor position of the H-2D^d peptide. These polymorphisms are buried in the antigen binding groove and can therefore not be directly contacted by a receptor; they can only affect the bound peptide. However, it should be noted that even if recognition does not require a specific peptide, it is still peptide-dependent, and all peptides active in this respect contain the p2Gp3P motif (Correa and Raulet, 1995; Orihuela et al., 1996). The principal difference between H-2D^d and H-2D^b in this part of the molecule is that the p2Gp3P motif assumes a very specific conformation and is deeply buried (Figures 2 and 4). The corresponding peptide residues in H-2D^b or H-2K^b, both failing to bind Ly-49A, are variable among binding peptides (Rammensee et al., 1995), and the molecular profile toward the solvent is consequently variable and different from H-2D^d in this region. One possibility that reconciles available functional data with the structure presented here is that the peptide may provide specificity not by exposing certain residues that can be engaged by the receptor but rather by avoiding exposure at positions 2 and 3, thereby also avoiding disturbance of receptor engagement close to this part of the groove.

Adjacent to this region, residues W73 and Y156 form a hydrophobic ridge in the H-2D^b peptide binding cleft that is absent in H-2D^d. This ridge is also missing in the other Ly-49A ligands, H-2D^p and H-2D^k, but is present in the nonbinding ligand H-2L^d (Balendiran et al., 1997). At the position of the ridge in H-2D^d there is a plateau, lined by the negatively charged D77 and D156 and the tryptophans in positions 97 and 114. The ridge may influence the binding of a receptor. In accordance with this notion, mutation of positions 73 and 156 in the H-2D^d molecule impaired protection against Ly-49A$^+$ cells, but only partially (Waldenström et al., 1998). The absence of this ridge is therefore not sufficient to allow Ly-49A binding. This is also supported by the fact that this ridge is lacking in H-2K^b, which is not recognized by Ly-49A. Continuous to this area is a region where H-2D^d and H-2D^b differ significantly with contributions from the α_1 as well as the α_2 domains, including the variable residues 73, 77, 80, 81, 83, 119, and 121 (Figure 5). Some residues of this region in the human (73, 77, and 80) are important for the binding of immunoglobulin-like KIR (killer inhibitory receptors) molecules (Colonna et al., 1993a, 1993b; Cella et al., 1994; Gumperz et al., 1995; Luque et al., 1996).

The second region of interest for Ly-49A recognition lies beneath the α_2-helix but is well exposed to the solvent. It contains a cluster of residues (2, 103, 104, 107, and 169) that differ between H-2D^d and H-2D^b and that form a loop in the N-terminal part of the α_2-domain of the H-2D^d structure. This region is near the glycosylation site at N176. There is evidence that the carbohydrate at this site can contribute to binding by Ly-49A, even if it does not appear to be necessary for functional recognition and inhibition (Matsumoto et al., 1998).

Conclusions

The crystal structure of the H-2D^d/RGPGRAFVTI complex resolved at 2.4 Å reveals a cleft with one deep and narrow part, where the tandem anchor position p2Gp3P fits snugly with minimal solvent exposure, and one shallow and broad part, where the C-terminal half of the peptide protrudes and is readily exposed before it anchors deeply in the F pocket. The peptide first arches over a mid-cleft tryptophan wall and then further over the buried side chain of the secondary anchor position p5R. In the case of P18-I10, residues p5R-p8V form a type I′ reverse turn, exposing positions 6–9, particularly p7F, to the T cell receptor. These results are consistent with several observations in functional studies of T cells recognizing the P18-I10 peptide. In addition, the structural analysis suggests a motif comprising p7F and conserved residues in the α_1 domain as a possible explanation for CTL clones that can recognize the peptide whether it is presented by H-2D^d or H-2D^p. Previous functional studies of NK cells have indicated that allelic specificity of the Ly-49A inhibitory receptor may be determined by polymorphisms in the N-terminal part of the α_2-domain of H-2D^d. Based on the structure, we propose two regions of interest in this respect, where H-2D^d and H-2D^b (not recognized by Ly-49A) differ in structural motifs: (1) the N-terminal part of the peptide binding cleft, where most H-2D^d complexes, irrespective of peptide content, should be similar due to low solvent exposure of the peptide; and (2) an exposed loop beneath the α_2-helix. The role of these regions may be explored by site-directed mutagenesis.

Table 2. Data Collection and Refinement Statistics

Data collection	
Resolution (Å)	25.0–2.4
Measured reflections	199263
Unique reflections	20963
Completeness (%)	
All data	96.5
Highest resolution shell (2.46–2.40 Å)	94.6
R_{Merge} (%)	
All data	4.0
Highest resolution shell	29.8
$I/\sigma(I)$	
All data	34.0
Highest resolution shell	4.7
Mosaicity (°)	0.61
Refinement Statistics	
Resolution (Å)	20.0–2.4
Unique reflections	17675
R_{cryst} (%)	29.3 (27.8)[a]
R_{free} (%)	33.8 (32.3)[a]
No. of protein atoms	3146
No. of waters	65
Average B-factor (Å^2)	
Protein	63.4
Peptide	50.8
Water	56.6
R.m.s. deviation, angles (°)	2.0
R.m.s. deviation, bonds (Å)	0.009
R.m.s. B-factor (Å^2)	
Main chain	1.6
Side chain	1.3
Ramachandran plot (%)	
Residues in most favored regions	86.9
Residues in disallowed regions	0

[a]Values in parentheses are calculated for the resolution interval 6.0–2.4 Å.

Experimental Procedures

Data Collection and Processing

Cloning, refolding, and crystallization of the MHC class I molecule H-2D^d complexed with the HIV-1 peptide RGPGRAFVTI from the V3 loop of the gp160 (sequence corresponding to HXB2R, LAI, and NL43 strains; Korber et al., 1997) have already been described (Achour et al., 1998). Crystals of the H-2D^d complex belong to space group $P2_12_12_1$ with cell dimensions a = 51.3 Å, b = 92.5 Å, and c = 108.8 Å. The first data set was collected at room temperature using a Rigaku rotating anode. The following data collection was performed under cryogenic conditions (T = 100K), to 2.6 Å resolution at beamline X11, EMBL outstation, DESY, Hamburg (λ = 0.910 Å) and to 2.4 Å resolution at beamline BM14, ESRF, Grenoble (λ = 0.900 Å). In all cases, a MAR research imaging plate system was used. The diffraction data was indexed with the DENZO program and scaled in SCALEPACK (Otwinowski, 1993). The space group was determined with DENZO in combination with the PATTERN program (Lu, 1996). Data collection statistics for the data set used in the final refinement are presented in Table 2.

Structure Determination and Refinement

The structure of the H-2D^d complex was solved by molecular replacement using the AMoRe program (Navaza, 1994). The H-2K^b-OVA crystal structure (Fremont et al., 1995), with the peptide omitted, was used as a search model. The rotation and translation search gave one single solution at α = 152.95°, β = 64.25°, and γ = 115.09°, T_x = 0.166, T_y = 0.303, and T_z = 0.341 with a correlation coefficient of 44.9. A rigid body refinement in XPLOR (Brünger, 1989), treating the heavy and the β_2m chains as separate units, gave an R factor of 45.9% for data in the 8–3.0 Å resolution interval. The model was rebuilt with the amino acid sequence of H-2D^d using the O program (Jones et al., 1991). A new data set to 2.6 Å resolution collected at the EMBL outstation in Hamburg was used for further refinement. 7% of the reflections were set aside for monitoring the refinement by R_{free} (Brünger, 1992). During refinement, extensive use of σA weighted difference electron density maps and also omit maps was made. Throughout refinement, all reflection data were used without any σ-cutoff. After simulated annealing using XPLOR (Brünger, 1989), the model was rebuilt, where relevant. A clear difference electron density was observed in the peptide binding cleft, and the peptide RGPGRAFVTI could be placed unambiguously. The model was further refined by positional refinement, resulting in an R_{free} of 36.8%. At this point, a new data set to 2.4 Å resolution collected at the ESRF in Grenoble became available. The reflections for monitoring R_{free} were kept the same as in the previous data set and refinement was continued with Refmac (Murshudov et al., 1997), including a bulk solvent correction, isotropic B factor refinement for atoms, and anisotropic overall B factor refinement on the reflection data. The mean B value resulting from the refinement, 63 Å^2, agrees well with that obtained from Wilson plots calculated for all three data sets, 60, 64, and 67 Å^2, respectively. Water molecules were included manually at significant positive electron densities (3σ in the F_o-F_c map). The final rounds of refinement were carried out using data from 20 to 2.4 Å yielding R_{cryst} = 29.3% and R_{free} = 33.8% (27.8 and 32.3 in the resolution shell 6.0 - 2.4 Å). In spite of these relatively high R factors that might reflect inherent disorder in the crystals as indicated by their high B factors, the electron density map was of very good quality. The overall real space correlation coefficient (Jones et al., 1991) of the model to the final 2 F_o-F_c electron density map was 0.82. The stereochemistry of the model was analyzed with PROCHECK (Laskowski et al., 1993). Solvent accessible areas were analyzed with the programs areaimol/resarea contained in the CCP4 suite (Collaborative Computational Project No. 4, 1997). Refinement statistics are given in Table 2.

Acknowledgments

We are greatful for access to synchrotron time at the EMBL outstation, beamline X11, DESY, Hamburg, and at the ESRF, beamline

BM14, Grenoble. We thank T. Sandalova, E. Morgunova, and E. Johansson for assistance with collection of crystallographic data, C.-I. Bränden, M. Norin, and P.-O. Campos De Lima for helpful discussions, and M. Alheim-Olsson for sharing unpublished data. This work has been supported by grants from the Swedish Cancer Society (K. K. and C. L. S.), the Swedish Medical Research Council, project number 11598 and 11324 (C. L. S.), and the Karolinska Institute (G. S.).

Received April 27, 1998; revised July 22, 1998.

References

Abastado, J.-P., Jaulin, C., Schutze, M.-P., Langlade-Demoyen, F., Plata, F., Ozato, K., and Kourilsky, P. (1987). Fine mapping of epitopes by intradomain recombinants. J. Exp. Med. *166*, 327–340.

Achour, A., Harris, R.A., Persson, K., Sundbäck, J., Sentman, C.L., Schneider, G., Lindqvist, Y., and Kärre, K. (1998). Murine MHC class I H-2D^d complex: expression, refolding and crystallisation. Acta Crystallogr., in press.

Alexander-Miller, M.A., Parker, K.C., Tsukui, T., Pendleton, C.D., Coligan, J.E., and Berzofsky, I.A. (1996). Molecular analysis of presentation by HLA-A2.1 of a promiscuously binding V3 loop peptide from the HIV-1 envelope protein to human cytotoxic T lymphocytes. Int. Immunol. *8*, 641–649.

Balendiran, G.K., Solheim, J.C., Young, A.C.M., Hansen, T.H., Nathenson, S.G., and Sacchettini, J.C. (1997). The three dimensional structure of an H-2L^d peptide complex explains the unique interaction of L^d with beta-2 microglobulin and peptide. Proc. Natl. Acad. Sci. USA *94*, 6880–6885.

Bjorkman, P.J., and Parham, P. (1990). Structure, function, and diversity of class I major histocompatibility complex molecules. Annu. Rev. Biochem. *59*, 253–288.

Bjorkman, P.J., Saper, M.A., Samraoui, B., Bennett, W.S., Strominger, J.L., and Wiley, D.C. (1987a). Structure of the human class I histocompatibility antigen, HLA-A2. Nature *329*, 506–512.

Bjorkman, P.J., Saper, M.A., Samraoui, B., Bennett, W.S., Strominger, J.L., and Wiley, D.C. (1987b). The foreign antigen binding site and T cell recognition regions of class I histocompatibility antigens. Nature *329*, 512–518.

Bouvier, M., and Wiley, D.C. (1994). Importance of peptide amino and carboxyl termini to the stability of MHC class I molecules. Science *265*, 398–402.

Brennan, J., Mager, D., Jefferies, W., and Takei, F. (1994). Expression of different members of the Ly-49 gene family defines distinct natural killer cell subsets and cell adhesion properties. J. Exp. Med. *180*, 2287–2295.

Brünger, A. (1989). Crystallographic refinement by simulated annealing: application to crambin. Acta Crystallogr. *A45*, 50–61.

Brünger, A. (1992). Free R value: a novel statistical quantity for assessing the accuracy of crystal structure. Nature *355*, 472–475.

Cella, M., Longo, A., Ferrara, G.B., Strominger, J.L., and Colonna, M. (1994). NK3-specific natural killer cells are selectively inhibited by Bw4-positive alleles with isoleucine 80. J. Exp. Med. *180*, 1235–1241.

Collaborative Computational Project No.4 (1994). The CCP4 suite: programs for protein crystallography. Acta Cryst. *D50*, 760–773.

Colonna, M., Borsellino, G., Falco, M., Ferrara, G.B., and Strominger, J.L. (1993a). HLA-C is the inhibitory ligand that determines dominant resistance to lysis by NK1- and NK2-specific natural killer cells. Proc. Natl. Acad. Sci. USA *90*, 12000–12004.

Colonna, M., Brooks, E.G., Falco, M., Ferrara, G.B., and Strominger, J.L. (1993b). Generation of allospecific natural killer cells by stimulation across a polymorphism of HLA-C. Science *260*, 1121–1124.

Corr, M., Boyd, L.F., Padlan, E.A., and Margulies, D.H. (1993). H-2D^d exploits a four residue peptide binding motif. J. Exp. Med. *178*, 1877–1892.

Correa, I., and Raulet, D.H. (1995). Binding of diverse peptides to MHC class I molecules inhibits target cell lysis by activated natural killer cells. Immunity *2*, 61–71.

Daniels, B.F., Karlhofer, F.M., Seaman, W.E., and Yokoyama, W.M. (1994a). A natural killer cell receptor specific for a major histocompatibility complex class I molecule. J. Exp. Med. *180*, 687–692.

Daniels, B.F., Nakamura, M.C., Rosen, S.D., Yokoyama, W.M., and Seaman, W.E. (1994b). Ly-49A, a receptor for H-2D^d, has a functional carbohydrate recognition domain. Immunity *1*, 785–792.

Evans, S.V. (1993). SETOR: hardware-lighted three-dimensional solid model representations of macromolecules. J. Mol. Graph. *11*, 134–138.

Falk, K., Rotzschke, O., Stevanovic, S., Jung, G., and Rammensee, H.G. (1991). Allele-specific motifs revealed by sequencing of self-peptides eluted from MHC molecules. Nature *351*, 290–296.

Fremont, D.H., Stura, E.A., Matsumura, M., Peterson, P.A., and Wilson, I.A. (1995). Crystal structure of an H-2K^b-ovalbumin peptide complex reveals the interplay of primary and secondary anchor positions in the major histocompatibility complex binding groove. Proc. Natl. Acad. Sci. USA *92*, 2479–2483.

Gao, G.F., Tormo, J., Gerth, U.C., Wyer, J.R., McMichael, A.J., Stuart, D.I., Bell, J.I., Jones, E.Y., and Jakobsen, B.K. (1997). Crystal structure of the complex between human CD8$\alpha\alpha$ and HLA-A2. Nature *387*, 630–634.

Garboczi, D.N., Ghosh, P., Utz, U., Fan, Q.R., Biddison, W.E., and Wiley, D.C. (1996). Structure of the complex between human T-cell receptor, viral peptide and HLA-A2. Nature *384*, 134–141.

Garcia, K.C., Degano, M., Stanfield, R.L., Brunmark, A., Jackson, M.R., Peterson, P.A., Teyton, L., and Wilson, I.A. (1996). An $\alpha\beta$ T cell receptor structure at 2.5 Å and its orientation in the TCR-MHC complex. Science *274*, 209–219.

Gumperz, J.E., and Parham, P. (1995). The enigma of the natural killer cell. Nature *378*, 245–248.

Gumperz, J.E., Litwin, V., Phillips, J.H., Lanier, L.L., and Parham, P. (1995). The Bw4 public epitope of HLA-B molecules confers reactivity with natural killer clones that express NKB1, a putative HLA receptor. J. Exp. Med. *181*, 1133–1144.

Haskins, K., Kappler, J., and Marrack, P. (1984). The major histocompatibility complex-restricted antigen receptor on T cells. Annu. Rev. Immunol. *2*, 51–66.

Jones, Y.E. (1997). MHC class I and class II structures. Curr. Opin. Immunol. *9*, 75–79.

Jones, T.A., Zou, J.Y., Cowan, S., and Kjeldgaard, M. (1991). Improved methods for building protein models in electron density maps and location of errors in these models. Acta Crystallogr. *A47*, 110–119.

Kane, K.P. (1994). Ly-49 mediates EL4 lymphoma adhesion to isolated class I major histocompatibility complex molecules. J. Exp. Med. *179*, 1011–1015.

Karlhofer, F.M., Ribaudo, R.K., and Yokoyama, W.M. (1992). MHC class I alloantigen specificity of Ly-49$^+$ IL-2-activated natural killer cells. Nature *358*, 66–70.

Kärre, K. (1985). Role of target histocompatibility antigens in regulation of natural killer activity, a reevaluation and a hypothesis. In Mechanisms of Cytotoxicity by NK cells, Heberman, R.B., and Callawaert, D.M., eds. (New York: Academic Press), pp. 81–91.

Kärre, K., Ljunggren, H.-G., Piontek, G., and Kiessling R. (1986). Selective rejection of H-2-deficient lymphoma variants suggests alternative immune defence strategy. Nature *319*, 675–678.

Korber, B., Foley, B., Leitner, T., McCutchan, F., Hahn, B., Mellors, J.W., Myers, G., and Kuiken, C. (1997). Human Retroviruses and AIDS. A Compilation and Analysis of Nucleic and Amino Acid Sequences. Theoretical Biology and Biophysics. (Los Alamos, NM: Los Alamos National Lab).

Kraulis, P.J. (1991). MOLSCRIPT: a program to produce both detailed and schematic plots of protein structure. J. Appl. Cryst. *24*, 946–950.

Laskowski, R.J., Macarthur, W., Moss, D., and Thornton, J. (1993). Procheck: a program to check stereochemical quality of protein structures. J. Appl. Crystallogr. *26*, 283–290.

Litwin, V., Gumperz, J.E., Parham, P., Philips, J.H., and Lanier, L.L. (1994). NKB1: a natural killer cell receptor involved in the recognition of polymorphic HLA-B molecules. J. Exp. Med. *180*, 537–543.

Ljunggren, H.G., and Kärre, K. (1990). In search of the "missing

self": MHC molecules and NK cell recognition. Immunol. Today *11*, 237–244.

Long, E.O., Burshtyn, D.N., Clark, W.P., Peruzzi, M., Rajagopalan, S., Rojo, S., Wagtmann, N., and Winter, C.C. (1997). Killer cell inhibitory receptors: diversity, specificity, and function. Immunol. Rev. *155*, 135–144.

Lu, G. (1996). A www service system for automatic comparison of protein structures. Protein Data Bank Quarterly Newsletter *78*, 10–11.

Luque, I., Solana, R., Galiani, M.D., Gonzalez, R., Garcia, F., Lopez de Castro, J.A., and Pena, J. (1996). Threonine 80 on HLA-B27 confers protection against lysis by a group of natural killer clones. Eur. J. Immunol. *26*, 1974–1977.

MacArthur, M.W., and Thornton, J.M. (1991). Influence of proline residues on protein conformation. J. Mol. Biol. *218*, 397–412.

Madden, D.R. (1995). The three-dimensional structure of peptide-MHC complexes. Annu. Rev. Immunol. *13*, 587–622.

Matsumoto, N., Ribaudo, R.K., Abastado, J.-P., Margulies, D.H., and Yokoyama, W.M. (1998). The lectin-like NK cell receptor Ly-49A recognizes a carbohydrate-independent epitope on its MHC class I ligand. Immunity *8*, 245–254.

Moretta, A., Vitale, M., Bottino, C., Orengo, A.M., Morelli, L., Augugliaro, R., Barbaresi, M., Ciccone, E., and Moretta, L. (1993). p58 molecules as putative receptors for major histocompatibility complex (MHC) class I molecules in human natural killer (NK) cells. Anti p58 antibodies reconstitute lysis of MHC class I protected cells in NK clones displaying different specificities. J. Exp. Med. *178*, 597–604.

Murshudov, G.N., Vagin, A.A., and Dodson, E.J. (1997). Refinement of macromolecular structures by the maximum-likelihood method. Acta Crystallogr. *D53*, 240–255.

Navaza, J. (1994). AMoRe: an automated package for molecular replacement. Acta Cryst. *A50*, 157–163.

Nicholls, A., Sharp, K.A., and Honig, B. (1991). Protein folding and association: insights from the interfacial and thermodynamic properties of hydrocarbons. Proteins *11*, 281–296.

Orihuela, M., Margulies, D.H., and Yokoyama, W.M. (1996). The natural killer cell receptor Ly-49A recognizes a peptide-induced conformational determinant on its major histocompatibility complex class I ligand. Proc. Natl. Acad. Sci. USA *93*, 11792–11797.

Otwinowski, Z. (1993). Oscillation data reduction program. In Data Collection and Processing, L.Sawyer, N.Issacs, and S. Bailey, eds. (Warrington, United Kingdom: Daresbury Laboratory), pp. 55–62.

Rammensee, H.-G., Friede, T., and Stevanovic, S. (1995). MHC ligands and their peptide motifs: first listing. Immunogenetics *41*, 178–228.

Ryan, J.C., and Seaman, W.E. (1997). Divergent functions of lectin-like receptors on NK cells. Immunol. Rev. *155*, 79–89.

Sentman, C.L., Olsson, M.Y., Höglund, P., Lendahl, U., and Kärre, K. (1994). H-2 allele-specific protection from NK cell lysis in vitro for lymphoblasts but not tumour targets: protection mediated by α_1/α_2 domains. J. Immunol. *153*, 5482–5490.

Shirai, M., Pendleton, C.D., and Berzofsky, J.A. (1992). Broad recognition of cytotoxic T cell epitopes from the HIV-1 envelope protein with multiple class I histocompatibility molecules. J. Immunol. *148*, 1657–1667.

Shirai, M., Vacchio, M.S., Hodes, R.J., and Berzofsky, J.A. (1993). Preferential Vβ usage by cytotoxic T cells cross-reactive between two epitopes of HIV-1 gp160 and degenerate in class I MHC restriction. J. Immunol. *151*, 2283–2295.

Shirai, M., Kurokohchi, K., Pendleton, C.D., Arichi, T., Boyd, L.F., Takahashi, H., Margulies, D.H., and Berzofsky, J.A. (1996). Reciprocal cytotoxic T lymphocyte cross-reactivity interactions between two major epitopes within HIV-1 gp160. J. Immunol. *157*, 4399–4411.

Shirai, M., Kozlowski, S., Margulies, D.H., and Berzofsky, J.A. (1997). Degenerate MHC restriction reveals the contribution of class I molecules in determining the fine specificity of CTL recognition of an immunodominant determinant of HIV-1 gp160 V3 loop. J. Immunol. *158*, 3181–3188.

Sundbäck, J., Nakamura, M.C., Waldenström, M., Niemi, E.C., Seaman, W.E., Ryan, J.C., and Kärre, K. (1998). The α_2 domain of H-2D^d restricts the allelic specificity of the murine NK cell inhibitory receptor Ly-49A. J. Immunol. *160*, 5971–5978.

Takahashi, H., Houghten, R., Putney, S.D., Margulies, D.H., Moss, B., Germain, R.N., and Berzofsky, J.A. (1989a). Structural requirements for class I MHC molecule-mediated antigen presentation and cytotoxic T cell recognition of an immunodominant determinant of the human immunodeficiency virus envelope protein. J. Exp. Med. *170*, 2023–2035.

Takahashi, H., Merli, S., Putney, S.D., Houghten, R., Moss, B., Germain, R.N., and Berzofsky, J.A. (1989b). A single amino acid interchange yields reciprocal CTL specificities for HIV-1 gp160. Science *246*, 118–121.

Takahashi, H., Nakagawa, Y., Pendleton, C.D., Houghten, R., Yokomuro, K., Germain, R.N., and Berzofsky, J.A. (1992). Induction of broadly cross-reactive cytotoxic cells recognizing an HIV-1 envelope determinant. Science *255*, 333–336.

Takei, F., Brennan, J., and Mager, D.L. (1997). The Ly-49 family: genes, proteins and recognition of class I MHC. Immunol. Rev. *155*, 67–77.

Takeshita, T., Takahashi, H., Kozlowski, S., Ahlers, J.D., Pendleton, C.D., Moore, R.L., Nakagawa, Y., Yokomuro, K., Fox, B.S., Margulies, D.H., et al. (1995). Molecular analysis of the same HIV peptide binding to both a class I and a class II MHC molecule. J. Immunol. *154*, 1973–1986.

Townsend, A.R., Rothbard, J., Gotch, F.M., Bahadur, G., Wraith, D., and McMichael, A.J. (1986). The epitopes of influenza nucleoprotein recognized by cytotoxic T lymphocytes can be defined with short synthetic peptides. J. Exp. Med., *44*, 959–968.

Waldenström, M., Sundbäck, J., Olsson-Alheim, M.Y., Achour, A., and Kärre, K. (1998). Impaired MHC class I (H-2D^d)-mediated protection against Ly-49A$^+$ NK cells after amino acid substitutions in the antigen binding cleft. Eur. J. Immunol., in press.

Watts, S., Wheeler, C., Morse, R., and Goodenow, R.S. (1989). Amino acid comparison of the class I antigens of mouse major histocompatibility complex. Immunogenetics *30*, 390–392.

Wilmot, C.M., and Thornton, J.M. (1990). β-turns and their distortions: a proposed new nomenclature. Prot. Eng. *3*, 479–493.

Young, A.C.M., Zhang, W., Sacchettini, J.C., and Nathenson, S.G. (1994). The three-dimensional structure of H-2D^b at 2.4Å resolution: Implications for antigen-determinant selection. Cell *76*, 39–50.

Young, A.C., Nathenson, S.G., and Sacchettini, J.C. (1995). Structural studies of class I major histocompatibility complex proteins: insights into antigen presentation. FASEB J. *9*, 26–36.

Zinkernagel, R.M., and Doherty, P.C. (1974). Restriction of in vitro T cell-mediated cytotoxicity in lymphotic choriomeningitis within a syngeneic or semiallogeneic system. Nature *248*, 701–702.

Brookhaven Protein Data Bank Accession Number

Atomic coordinates and structure factors for the H-2D^d/P18-I10 complex have been deposited with the accession code 1bii.